IEEE Access
Multidisciplinary ⋮ Rapid Review ⋮ Open Access Journal

Received 3 November 2023, accepted 22 November 2023, date of publication 28 November 2023,
date of current version 6 December 2023.

Digital Object Identifier 10.1109/ACCESS.2023.3337551

RESEARCH ARTICLE

GRLF-LAD Control Based Active Power Filter Operation With QSG-SOGI Algorithm for Grid Voltage Harmonics Disturbance Rejection

MASIHA AIJAZ[1], IKHLAQ HUSSAIN[1], (Senior Member, IEEE), SHAMEEM AHMAD LONE[1], (Member, IEEE), AND MUKUL CHANKAYA[2]

[1]Department of Electrical Engineering, National Institute of Technology Srinagar, Srinagar, Jammu and Kashmir 190006, India
[2]School of Electrical Engineering, Vellore Institute of Technology, Vellore Campus, Vellore, Tamil Nadu 632014, India

Corresponding author: Mukul Chankaya (mukul.chankaya@vit.ac.in)

This work was supported by the Vellore Institute of Technology, Vellore Campus, Tamil Nadu.

ABSTRACT This article presents application of generalized robust logarithmic family (GRLF) framework derived least absolute difference (LAD) Algorithm implemented for active power filters (APF) for PQ enhancement. The presented GRLF-LAD algorithm successfully eliminates lower as well as higher order errors from the harmonically rich nonlinear load currents and thus results in accurate fundamental component extraction. Weak power grids are characterised by distorted grid voltages and riddled with inherent harmonics. Conventional techniques such as synchronous reference frame (SRF) algorithm are unable to filter out the harmonics from grid voltages and this results in oscillations in D-Q components. This leads to generation of a distorted reference current and thus unsatisfactory APF performance. In this article, the grid voltages are processed by modified second-order generalized integrator with quadrature signal generator (QSG-SOGI) based algorithm. The harmonic rejection capabilty of QSG-SOGI is far superior than other tested algorithms. QSG-SOGI shows remarkable improvement of approximately 99.35% than SRF and 96.02% than SOGI in terms of percentage improvement. The performance of presented APF is verified experimentally on a developed prototype and tested rigorously against load variations, grid voltage variations as well as grid distortions. The GRLF-LAD algorithm is found to be approximately 36.04% faster than APA and about 45.16% faster than LMS in terms of dynamic response and about 11.19% better than LMS in accurate current component extraction. The total harmonic distortion (THD) content of presented algorithm is found to be well within the IEEE-519 std.

INDEX TERMS Power quality, active power filter, adaptive controls, polluted grid conditions, grid voltage harmonic reduction.

I. INTRODUCTION

Power converters have been established as a reliable technology for integrating energy sources, storage systems and essential loads into microgrids. However, with the influx of such power electronic converters, the nonlinear currents, thus emanating from such devices has also risen exponentially. When such devices, loads and machines are connected with the power grid, these create a range of power quality (PQ) issues such as harmonics in the grid current, waveform distortion, unbalance, reactive power drawn, fluctuations in voltages or/and currents in supply systems etc. Thus, it has become imperative to compensate such nonlinear loads so as to maintain unity power factor (UPF) at the grid side. APFs are established to compensate for PQ concerns, which have been demonstrated to work. APFs can be shunt connected [1], [2], series connected [3] or a combination of series and shunt APFs connected in back-to-back configuration and sharing a common DC link [4]. The extent of PQ enhancement is dependent on extrication of fundamental component of nonlinear currents of such loads, thereby eliminating the higher order harmonics. Various control algorithms have been

The associate editor coordinating the review of this manuscript and approving it for publication was Chi-Seng Lam.

developed in the literature to address this issue. Widely used control based on synchronous reference frame (SRF) theory [5] uses the transformation of quantities to the synchronous frame. The control algorithm utilises a low pass filter to minimize the second harmonic prevalent in the direct component of load current. However, although it shows better steady state response, SRF gives poor dynamic response during load variation [6].

Adaptive filtering algorithms have also been reported since they have rapid transient response [7]. In order to manage APF switching, [8] implements least mean square (LMS) algorithm adaptive filtering technique to extricate fundamental component of nonlinear load current. Several LMS derived algorithms have also been implemented in the literature [9], [10], [11], [12]. However, such algorithms require tuning of several variables simultaneously to generate accurate fundamental weight component. Higher order LMS such as least mean fourth (LMF) [13] and combined LMS-LMF based control [14] have been proposed in the literature to improve upon the sluggish convergence rate of LMS. Higher order LMS exhibit undesirable steady-state behaviour since even a minor inaccuracy is amplified. Additionally, generalised filter-based algorithms have been put out in the literature [15], [16], [17] utilises modified dual second order generalized integrator (MD-SOGI) as control technique, however, the effect of polluted grid conditions has not been studied. Furthermore, steepest descent laplacian regression (SDLR) based adaptive control technique from the affine projection family is presented for a photovoltaic (PV) array integrated, three phase system in [18]. The computational complexity of the laplacian network proves to be a hindrance in the real time implementation of the adaptive control based upon the number of harmonics chosen. Reference [19] utilises affine projection algorithm (APA) for fundamental component extraction however, it shows a sluggish response. The basic framework in learning theory generally considers learning from examples by optimizing (minimizing or maximizing) a certain loss function. Due to their mathematical tractability and simplicity, second order statistical measures like mean square error (MSE), variance, and correlation are frequently employed as loss functions in machine learning and adaptive system training. The loss functions based on the second order statistical measures, however, are sensitive to outliers in the data, and are not good solutions to learning with non-Gaussian data in general [20]. To handle non-Gaussian data (or noises), various non-second order loss functions are frequently applied to learning systems. Particularly in recent years, a novel similarity measure, called correntropy [21], has been successfully applied to robust learning and signal processing. By maximising the generalised correntropy, the generalised maximum correntropy criterion technique (GMCCT) was developed [22]. However, the GMCCT suffers from high computational cost of the generalised gaussian kernel calculation (exponential term) in its weight update equation. Huang et al. [23] utilises versoria function [24] as the cost function to maximise the cost function to develop maximum versoria criterion algorithm (MVCA). MVCA avoids the usage of exponential term which reduces computational effort and demonstrates robustness against errors of large amplitude. Furthermore, techniques that depend on logarithmic cost function [25] were developed in order to ease the computational burden and enhance the accuracy of the weight of the load component like novel robust least mean logarithmic square (RLMLS) [26] algorithm. A new class of algorithms based on generalized robust logarithmic family (GRLF) framework is developed by Abdelrhman et al. [27]. This article presents the application of GRLF-LAD algorithm to extract the fundamental component of nonlinear load currents. The algorithm combines the robustness of MVCA against impulsive noise as well as reduced complexity provided by RLMLS algorithm. The GRLF-LAD algorithm shows rapid response and accurate current component extraction and low THD content.

With increasing importance of decreasing carbon footprint, development of smart microgrids and nanogrid clusters with photovoltaic (PV), hydro, wind, hydrogen and battery storage integration have been gaining importance. However, such microgrid topologies also contribute to degradation of system PQ due to increasing usage of power electronic conversion devices at the POC. Thus, advanced control algorithms developed for APFs find their applicability in such energy sources integrated applications to mitigate PQ issues. Several works have explored the development of filters for various applications. In addition to PQ enhancement, the developed filters can have multiple functions such as elimination of the oscillations in the power injected to the grid, reactive power compensation etc. Singh et al. [28] proposes modified double-band HCC (MDBHCC) with proportional resonant (PR) controller for single-phase PV integrated systems. Smadi et al. [29] describes the development of a PV converter with built-in hybrid active power filtering (HAPF) features for cost-effective low order harmonic mitigation along with reactive compensation. Mishra and Lal [30] proposes a multi objective control scheme which improves PQ as well as enhances the low-voltage ride-through (LVRT) capability simultaneously during abnormal grid conditions for a three phase grid tied PV system. Tyagi et al. [31] develops control strategy for harmonic free power generation in hydro plants. Das and Singh [32] develops a ripple suppressing control filter for PV-wind energy integrated systems for smooth power injection even in unbalanced and distorted grid conditions.

In nations like India, distorted grid voltages are regular and widespread. If the system operates under perfect grid conditions, the most commonly implemented SRF has a very robust construction and can estimate the phase angle quickly. However, for a polluted grid voltage situation, oscillations are present in estimated voltage quantities and their derivatives [33]. In order to increase performance under less-than-ideal circumstances. These filters are used

to reduce the grid voltage harmonics' impact on the PLL. Some of these filters include adaptive notch filters [34], [35]. In order to mitigate oscillations of the grid D-Q voltages, SOGI based filtering approach is used, which has a better harmonic filtering performance than SRF. However, the extent of reduction of harmonic components is not adequate. This can lead to distorted unit template generation and peak of grid voltage estimation. In this article, the grid voltage processing is implemented by modified second-order generalized integrator (SOGI) with quadrature signal generator (QSG) [36]. The QSG-SOGI removes the residual harmonics which are not eliminated by SOGI filter and thus distortion free unit template generation is achieved. Following are the contributions overlaid in this article.

1) An APF for PQ enhancement is implemented in this article. IEEE 519 standard compliant control algorithm is designed for the APF. For the purpose of quickly extracting the fundamental component from the nonlinear load currents, GRLF-LAD control algorithm has been used. MATLAB Simulation results reveal that terms of steady state response, GRF-LAD is only approximately 0.40% worse than APA in weight generation, but it is about 11.19% better than LMS in weight generation.
2) The detrimental impacts of harmonically polluted and fluctuating grid voltages have been successfully removed by the QSG-SOGI based grid voltage component extraction. Under unexpected load disruptions, its accuracy and response time have been shown to be good. Comparison with SRF and SOGI algorithms depicts the THD from SRF is 12.37%, 2.1% from SOGI while the QSG-SOGI generates THD of only 0.08%. Thus, QSG-SOGI shows remarkable improvement of approximately 99.35% than SRF and 96.02% than SOGI in terms of percentage improvement.
3) The comparison of implemented control algorithm against other control algorithms provided in literature has been experimentally ratified. The robustness of the APF control algorithms during load variations and grid voltage abnormalities have been corroborated by experimental results. The GRLF-LAD algorithm is found to be approximately 36.04% faster than APA and about 45.16% faster than LMS in terms of dynamic response.

This work's remaining sections are organised as follows. The system topology is presented in Section II along with the design of components. Introduced in Section III is the suggested control method. The simulation results are presented in Section IV. The experiment's findings are presented in Section V. Section VI summarises the findings and Section VII brings this article to a close.

II. PROPOSED SYSTEM TOPOLOGY

The presented topology in Fig. 1 is used for the enhancement of the PQ for the distribution systems. The system comprises of a nonlinear load connected at the point of coupling (POC) which is supplied by single phase grid. The nonlinear load is modeled using diode bridge rectifier coupled with RL load to test the PQ enhancement capability of the APF. R_L and L_L are the load resistance and inductance parameters respectively. The grid impedance denoted by Z_s. To cut down on noise at high switching frequencies, ripple filters (R_f and C_f) are connected in shunt at the grid end. The interfacing inductors (L_i), which are connected in series to minimise ripples in the compensatory currents, i_c. The 4 switched, single phase voltage source converter (VSC) is connected at the POC with a DC link capacitor C_{DC} at the DC side. The acquisition of the voltage and current signals is handled by the VI sensing circuitry. These physical signals are converted for interfacing with the digital controller using analog to digital converters (ADC). The proposed algorithm for PQ improvement is generated by the MATLAB-dSPACE interface and is responsible for switching the VSC appropriately so as to present UPF mode during various dynamic conditions. The switching signals are passed through optocoupler and given to the gate driver circuit for the switching pulses generation of the VSC.

III. VSC CONTROL

Various controlling strategies that are used to produce VSC switching signals are covered in this section. These include the generation of distortion less unit vector sinusoids, the extraction of fundamental component from load currents, estimation of loss components of converter and generation of reference currents.

A. GENERATION OF DISTORTION LESS UNIT VECTOR SINUSOIDS

For the operation of VSC at UPF, the grid voltage unit vector are to be generated. In a polluted grid scenario, the grid voltages are affected by harmonics which is due to insufficient compensation or excess of nonlinear loads

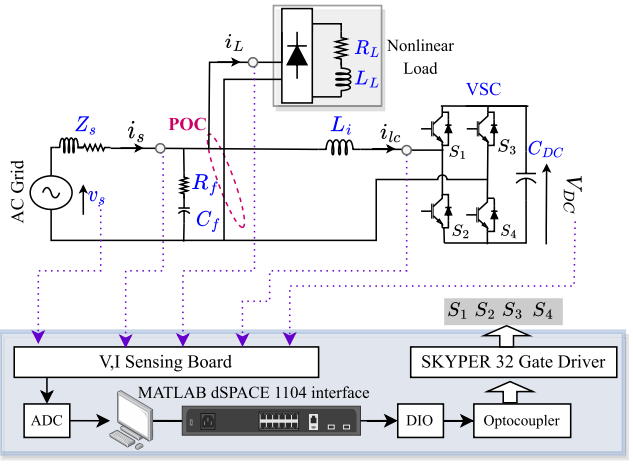

FIGURE 1. System configuration.

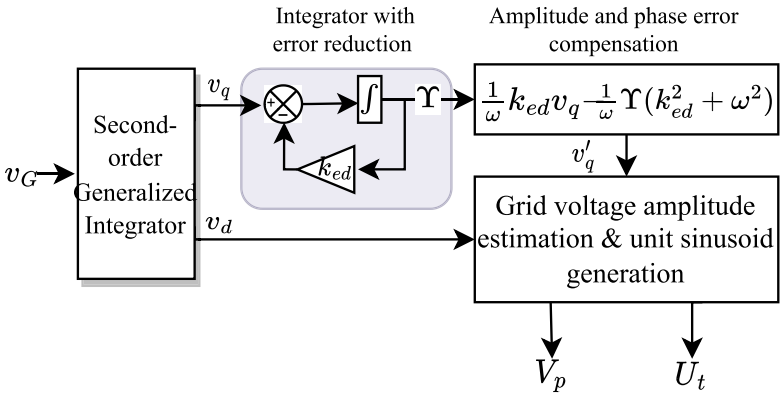

FIGURE 2. Structure of QSG-SOGI for distortion-less grid voltage processing.

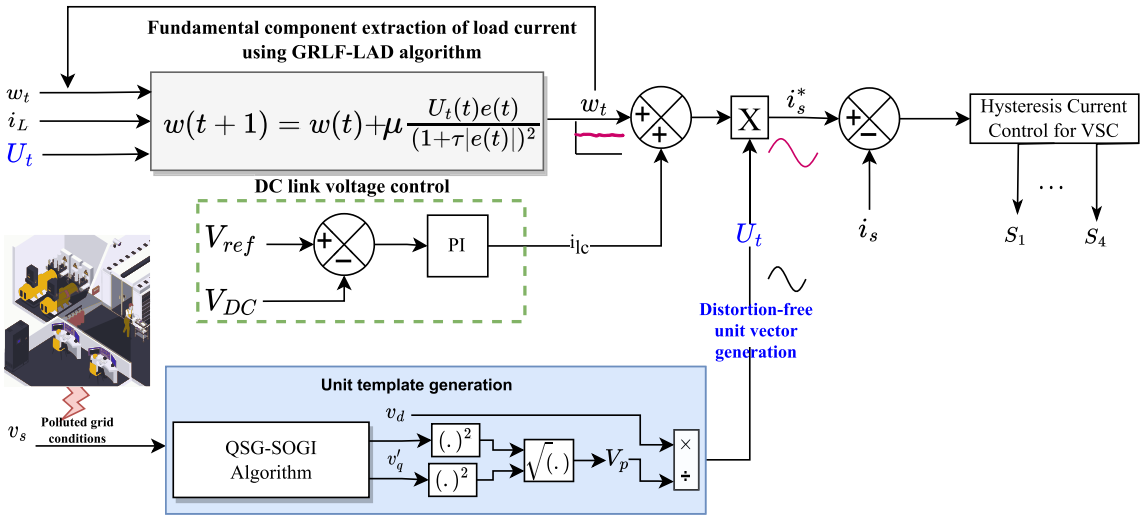

FIGURE 3. Detailed control strategy of the proposed system.

integrated with the power grid. As a result, the unit template which is to be generated from the grid voltages are distorted. These distorted unit vectors are then to be utilised in the reference current generation for the UPF mode of the VSC, which would, unsurprisingly result in inaccurate reference current which ultimately leads to inadequate compensation. To tackle this issue, extraction of distortion free unit templates using QSG-SOGI for oscillation reduction. As shown in Fig. 2, the integrator with an error-decaying mechanism acts as an low pass filter (LPF) with the following transfer function

$$\Upsilon = v_G \left(\frac{1}{s + k_{ed}} \right) \tag{1}$$

Amplitude, AM, and phase angle, θ_i, of the modified integrator in Eq. (1) is given as

$$AM = \left(\frac{1}{\sqrt{\omega^2 + k_{ed}^2}} \right)$$
$$\theta_i = -\tan^{-1}(\omega / k_{ed}) \tag{2}$$

where, ω is the estimated frequency of the PLL output. Assuming the input to the modified integrator, $q_v' = X_i sin(\omega t)$, then the output is given by

$$\Upsilon = \frac{X_i sin(\omega t + \theta_i)}{\sqrt{\omega^2 + k_{ed}^2}} \tag{3}$$

while, the desired distortion-free in-phase grid voltage component v_d' is

$$v_d' = X_i sin(\omega t + \pi/2) = X_i cos(\omega t) \tag{4}$$

Expression in Eq. (3) can be trigonometrically manipulated to

$$\frac{X_i}{\sqrt{\omega^2 + k_{ed}^2}} sin(\omega t + \theta_i) = \frac{X_i}{\sqrt{\omega^2 + k_{ed}^2}} [sin(\omega t) cos(\theta_i) + cos(\omega t) sin(\theta_i)] \tag{5}$$

From Eq. (3), we know that

$$cos(\theta_i) = \frac{k_{ed}}{\sqrt{\omega^2 + k_{ed}^2}}; \quad sin(\theta_i) = \frac{-\omega}{\sqrt{\omega^2 + k_{ed}^2}} \tag{6}$$

Eq. (5) can be written as

$$\Upsilon = v_q \times \frac{k_{ed}}{\sqrt{\omega^2 + k_{ed}^2}} - v_d' \times \frac{-\omega}{\sqrt{\omega^2 + k_{ed}^2}} \tag{7}$$

Therefore, the desired in-phase signal, v_d' is extracted

$$v_d' = v_q \times k_{ed}/\omega - \left(\omega^2 + k_{ed}^2\right) \Upsilon/\omega \tag{8}$$

The amplitude of grid voltage V_p is calculated in the following way

$$V_p = \sqrt{v_d'^2 + v_q^2} \tag{9}$$

where v_d' and v_q are the orthogonal components of the voltage.

Then, the in-phase unit vector sinusoid is calculated as

$$U_t = \frac{v_d'}{V_p} \tag{10}$$

B. ESTIMATION OF LOSS COMPONENT OF CONVERTER

In order to operate APF effectively and to users' preferences, the DC-link voltage, V_{DC} is controlled to a fixed reference value. The resultant difference of sensed voltage and the reference DC-link voltage, V_{ref} is supplied to a PI controller with k_{pV} serving as the proportional gain and k_{iV} serving as the integral gain. The output of the DC-link controller termed as converter loss component i_{lc}, is computed as

$$V_{de}(j) = V_{DC}^*(j) - V_{DC}(j-1) \tag{11}$$

$$i_{lc}(j+1) = i_{lc}(j) + k_{pV}\left(V_{de}(j) - V_{de}(j-1)\right) + k_{iV} V_{de}(j) \tag{12}$$

C. FUNDAMENTAL COMPONENT EXTRACTION OF NONLINEAR CURRENT

The control approach is shown in Figure 3. The nonlinear load currents with their inherent harmonic content and distortion introduces harmonics into the grid currents. These load currents can be decomposed into sum of load current component at fundamental frequency and load current components at rest of the frequency components. The basic framework in adaptive filtering techniques generally considers optimizing (minimizing or maximizing) a certain cost function. These techniques heavily depend on the choice of cost function. The following system is under consideration

$$i_L(t) = U_t(t)(w^0)^T + q(t) \tag{13}$$

where $i_L(t)$ is the current through the nonlinear load under consideration at instant t, q(t) is additive disturbance and the optimum weight vector is denoted by w^0. The system error equation is denoted as

$$\xi(t) = i_L(t) - w_t^T(t) U_t(t) \tag{14}$$

where $w_t(t)$ is the weight vector of the adaptive filter.

This article presents the application of GRLF-LAD algorithm to extract the fundamental component of nonlinear load currents. The algorithm combines the robustness of MVCA against impulsive noise as well as reduced complexity provided by RLMLS algorithm.

The generalised MVCA cost function can be defined as

$$J_{MVCA}(\xi(t)) = E\left[\frac{1}{1 + \tau|\xi(t)|^p}\right] \tag{15}$$

where $E[.]$ denotes the expectation operator, p is the shape parameter and $\tau \geq 0$ is a constant versoria parameter. The versoria function based on the gradient ascent has a faster convergence rate and thus, produces a lower steady-state error.

The RLMLS cost function is defined as

$$J_{RLMLS}(\xi(t)) = E\left[\frac{ln(1 + \tau|\xi(t)|^p}{\tau}\right] \tag{16}$$

For small ranges of error signals, MVCA is nonconvex while the RLMLS is nonconvex for greater values of error signals. Hence, a combination of these two functions is used to develop a GRLF framework. The standard GRLF framework is developed using

$$J(\xi(t)) = \frac{1}{\tau^2} E\left[\frac{1}{1 + \tau|\xi(t)|^p} + ln(1 + \tau|\xi(t)|^p)\right] \tag{17}$$

where p is the shape parameter and its value is set to unity. The main appealing properties of the cost function described in Eq. (17) is that it captures a higher order of errors that eliminates the higher frequency components of the load current which results in enhancement of the filtering performance characteristics while maintaining robustness property in impulsive noise environments. Employing the gradient ascent approach, the GRLF algorithm weight vector update equation is as follows

$$w_t(t+1) = w_t(t) + \mu \frac{|\xi(t)|^{2(p-1)}}{(1 + \tau|\xi(t)|^p)^2} u_t(t)\xi(t) \tag{18}$$

By setting $p = 1$, the resulting algorithm, is then, GRF-LAD algorithm. The GRF-LAD algorithm captures a higher order of errors and enhance the filtering performance. Thus, the weight equation is as follows

$$w_t(t+1) = w_t(t) + \mu \frac{u_t(t)\xi(t)}{(1 + \tau|\xi(t)|)^2} \tag{19}$$

D. GENERATION OF REFERENCE GRID CURRENTS

The magnitude of the resultant reference grid current is obtained from the sum of the fundamental weight of load current and converter loss component.

$$w_p = i_{lc} + w_t(t) \tag{20}$$

Finally, the reference grid current is generated using Eq. (20) and Eq. (10) as follows:

$$i_s^* = U_t \times w_p \tag{21}$$

The resultant of sensed i_s and i_s^*, thus obtained, are passed on to a hysteresis current controller which is responsible for the generation of switching pulses for the VSC.

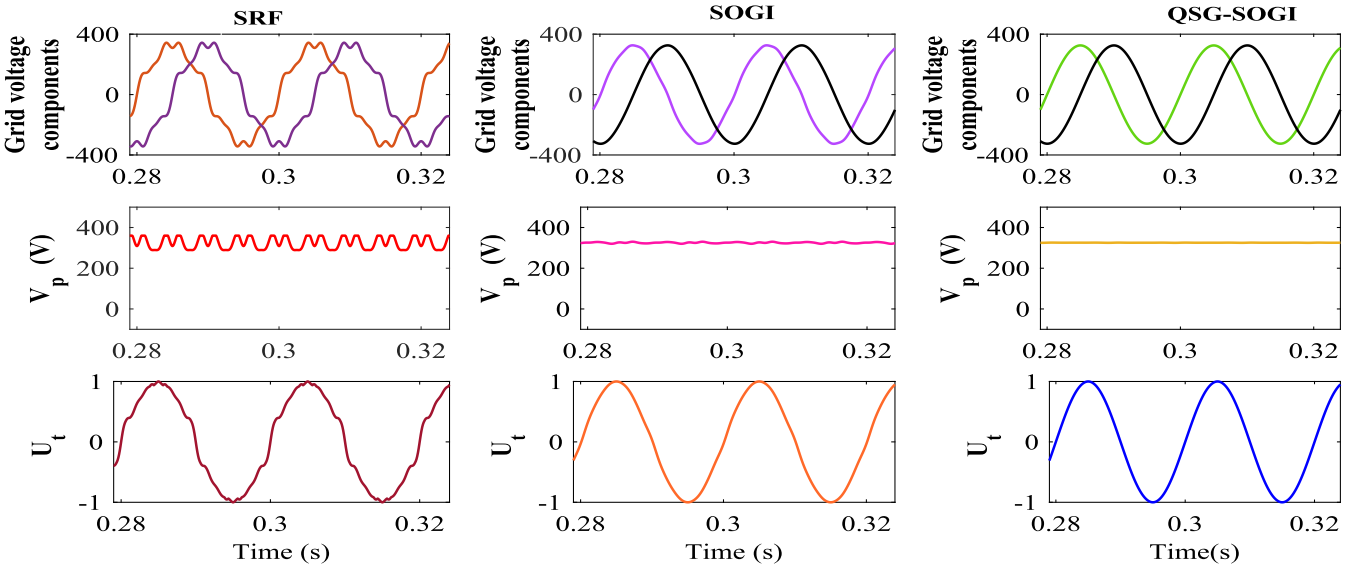

FIGURE 4. Comparative performance of control algorithms during voltage harmonic injection.

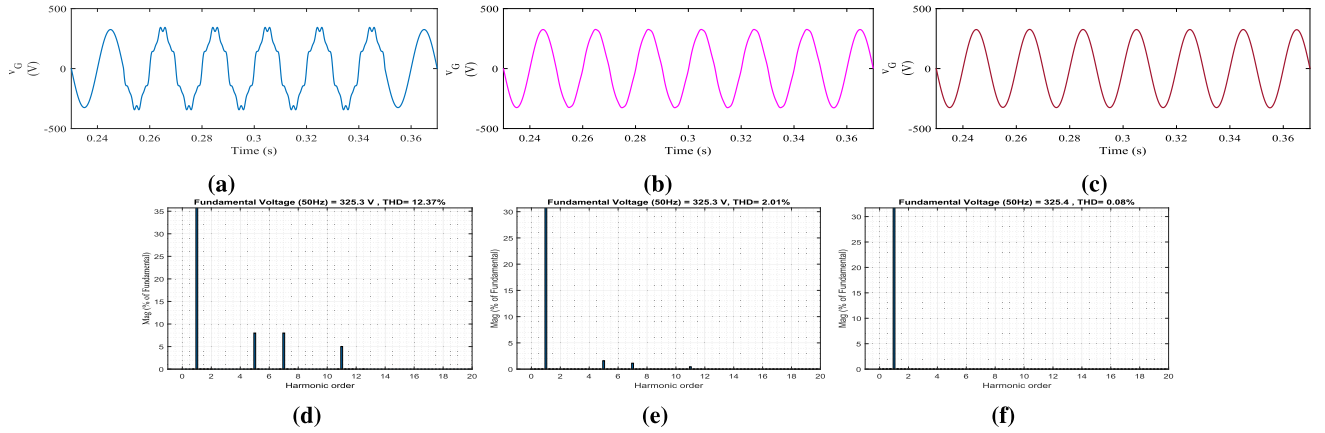

FIGURE 5. THD analysis of control algorithms (a) grid voltage THD using SRF. (b) grid voltage THD using SOGI. (c) grid voltage THD using QSG-SOGI.

IV. SIMULATION RESULTS

A. EVALUATION OF GRID VOLTAGE HARMONIC REJECTION CAPABILITY OF PROPOSED ALGORITHM

The comparison of SRF, SOGI and QSG-SOGI based control for accurate grid voltage processing for polluted grid voltage conditions is shown in Fig. 4. The control algorithm paramters are given in the appendix. From 0.25s to 0.35s, grid voltage is injected with harmonics to represent non-ideal polluted grid. The grid voltage harmonic pollution is represented by injecting 5th, 7th and 11th harmonic order frequencies of the magnitude 8%, 8% and 5% with respect to the fundamental grid voltage respectively. SRF control is unable to filter out harmonic injection which subsequently impacts the calculation of D-Q voltages. The distortion is therefore exhibited in generation of V_p. The SOGI control scheme's behaviour when the grid voltage is distorted is depicted. The amplitude of harmonics in the input voltage can often be eliminated due to the filtering effect of the SOGI. However, residual lower harmonic components produce oscillations in the grid DQ voltages. The QSG-SOGI based control eliminates the harmonic components by using a lower harmonic component of grid voltage which produces distortion free grid voltage components. Because of the aberrations in the grid voltage, both SRF and SOGI control systems function less well. The grid harmonic rejection capability in terms of THD analysis is shown in Fig. 5. The QSG-SOGI algorithm generated distortion-free voltage components, resulting in improvement in grid voltage THD. The THD from SRF is 12.37%, 2.1% from SOGI while the QSG-SOGI generates THD of only 0.08%. Thus, QSG-SOGI shows remarkable improvement of approximately 99.35% than SRF and 96.02% than SOGI in terms of percentage improvement. As evident, the QSG-SOGI successfully rejects all harmonics and significantly reduces all

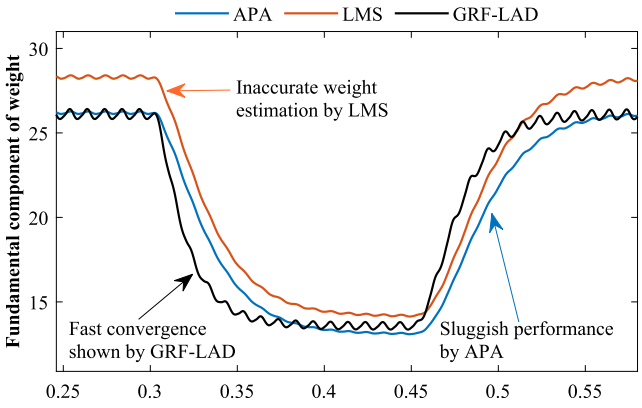

FIGURE 6. Comparative performance of control algorithms during load change.

the harmonics injected into the system, thus showing its efficacy.

B. EVALUATION OF FUNDAMENTAL COMPONENT EXTRACTION CAPABILITY OF PROPOSED ALGORITHM

The comparison of the fundamental component extraction capability of proposed algorithm is compared against APA and LMS algorithm. As seen in Fig. 6, the load current is suddenly decreased at 0.3s and increased again at 0.55s. The APA algorithm generates weight of 25.3 A which is accurate, however, it shows sluggish performance and shows slow transient performance. LMS algorithm produces inaccurate weight of 28.6A while GRF-LAD algorithm generates a weight component of 25.4 A. Thus, GRF-LAD is only approximately 0.40% worse than APA in weight generation, but it is about 11.19% better than LMS in weight generation and shows fast convergence than the other two algorithms.

V. EXPERIMENTAL VALIDATION

A prototype and experimental setup system of the grid integrated single phase APF is developed for experimental verification and the picture of the experimental setup is presented in Fig. 7 in order to confirm the viability of the proposed scheme. A single-phase autotransformer is used to realise an a single phase grid. To collect voltage and current signals, the signal collecting circuit employs Hall Voltage sensors (LV 25-P) and Hall Current sensors (LA 55-P). The VSC, which serves as the heart of the system, is implemented in hardware by using a Semikron inverter module with an IGBT SKM50GB12T4 as the primary circuit switching component. A DC auxiliary power supply also powers the signal gathering circuit and IGBT driving circuit. The signal sensing circuit collects signals, which are delivered to the ADC, where they are computed by dSPACE 1104. Then the switching signals are sent out through Skyper-32 gate drivers to the IGBT modules. The Tektronix oscilloscope is used to see the waveforms while the Fluke 125-B power quality analyzer is used to analyse the power quality and harmonic spectrum.

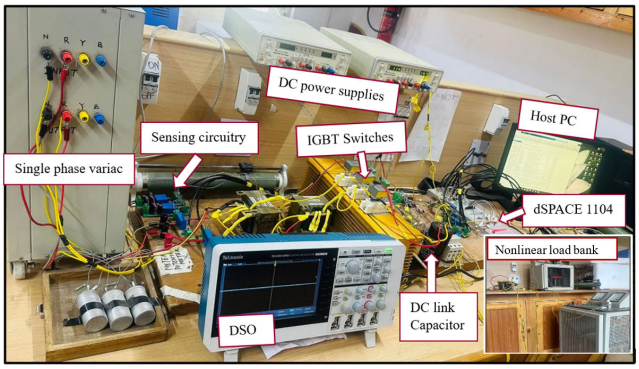

FIGURE 7. Experimental prototype.

A. STEADY STATE RESPONSE WITH NONLINEAR LOAD

The steady state behaviour of APF operation on the power quality can be observed in Fig. 8. Fig. 8a presents the waveforms of v_G and i_s. As depicted by Fig. 8 (b)-(d), the THD of v_G is 3.49% and i_s is 4.4% which is well within 5% limit as dictated by IEEE 519- std. THD of i_L is 23%. Fig. 8e presents the waveforms of v_L and i_L. Fig. 8(f)-(h) shows the power delivered by the grid, power delivered to the nonlinear load, and converter power. Thus, it can be observed that operation of APF enables a near unity power factor at the grid.

B. DYNAMIC RESPONSE OF THE SYSTEM UNDER NONLINEAR LOAD VARIATIONS

Fig. 9(a)-(b) depicts the system's behaviour when the load is disconnected. Fig. 9a shows the waveformS of i_L, w_t, err and i_{lc}. As soon as load is disconnected, i_L reduces to zero. Subsequently, w_t also decreases to zero. Fig. 9b presents waveforms of i_c, U_t, V_t and V_{DC}. With the load disconnected, i_c reduces to zero. Since, U_t and V_t are dependent entirely on v_G, the signals remain unaffected. With the load disconnected, V_{DC} rises slightly to maintain the power balance. Similar response can be seen in Fig. 9 (c) and (d) when nonlinear load is reinjected.

C. DYNAMIC PERFORMANCE UNDER GRID VOLTAGE DISTURBANCE

Fig. 10 (a) and (b) shows the system performance during voltage sag. The grid voltage is reduces from 40 V to 25 V. As depicted in Fig. 10a, v_G reduces and correspondingly i_s and i_L is reduced. V_{DC} is maintained. In Fig. 10b,, waveforms of i_s^*, w_t, V_t and V_{DC} are presented. With the voltage sag introduced in the system, the i_{sref} is also reduced in magnitude, however, the reference generated is still sinusoidal. Correspondingly w_t being adaptive in nature, is also reduced. V_t is also reduced accordingly. Similarly, the system performance is studied when voltage swell is introduced in the system as depicted in Fig. 10c-(d). Thus, it can be observed that the system maintains UPF even during

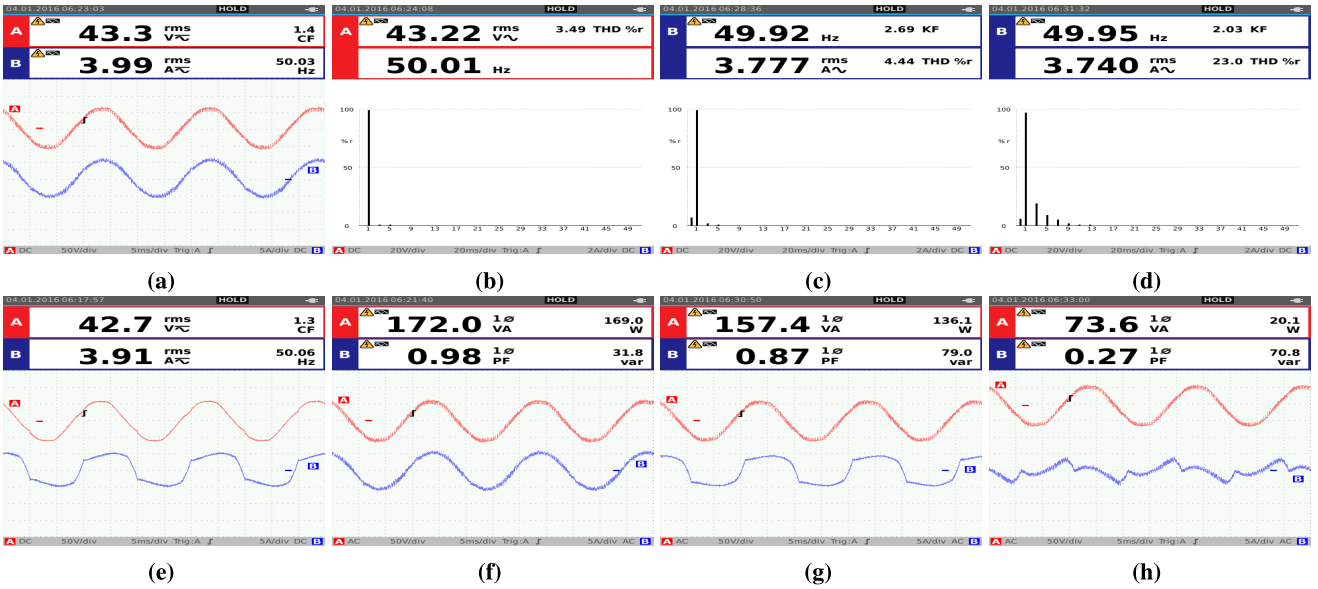

FIGURE 8. Steady state behaviour, (a) v_g and i_s. (b) Harmonic content of v_g. (c) Harmonic content of i_s. (d) Harmonic content of i_L. e) v_L and i_L. f) Utility power. g) Load power. h) Converter power.

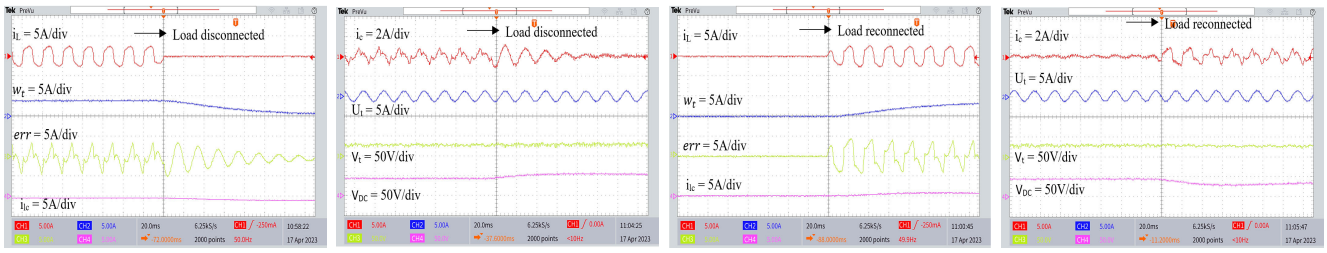

FIGURE 9. Comparative analysis of control algorithms during disconnection and reinjection of local nonlinear loads.

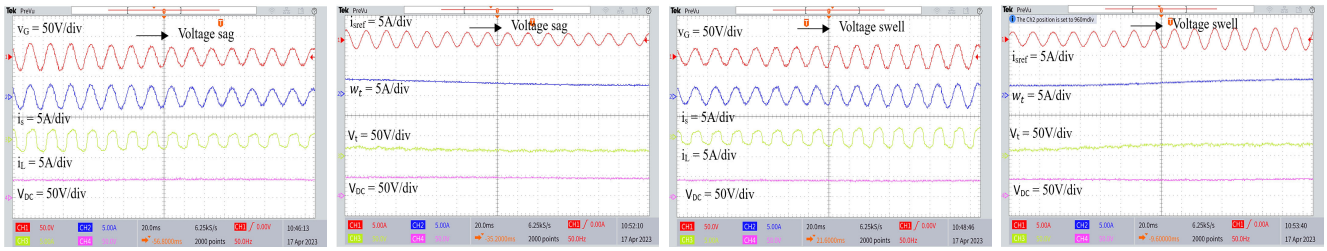

FIGURE 10. Dynamic performance with grid voltage variation, (a) and (b) during voltage sag, (c) and (d) during voltage swell.

sag and swell conditions, with i_s being sinusoidal and V_{DC} being maintained.

D. BEHAVIOR OF THE SYSTEM AS DSTATCOM SWITCHED-IN

Fig. 11 shows the system response as the APF is switched on. Fig. 11a depicts grid voltage, v_G, grid current i_s, nonlinear load current i_L and compensating current i_c. Initially, i_s is emulating i_L, however, as soon as APF commences operation, i_s becomes sinuosidal. Figure 11b depicts converter loss component i_{lc}, weight of fundamental component of i_L, w_t, V_t and V_{DC}. As it can be seen from the waveforms, the sytsem parameters remain constant inspite of transitioning to APF operation.

E. COMPARATIVE ANALYSIS OF CONTROL ALGORITHMS

Fig. 12 depicts the performance of the proposed GRLF-LAD adaptive control against other control algorithms [8], [19]

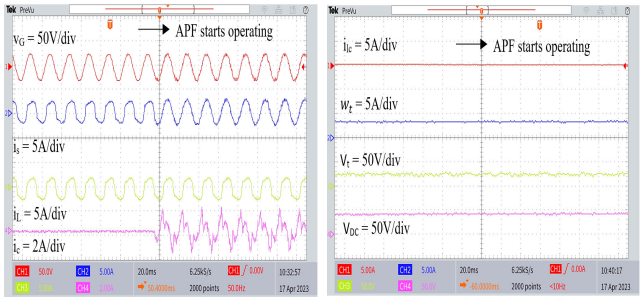

(a) (b)

FIGURE 11. System behaviour during APF turn-on.

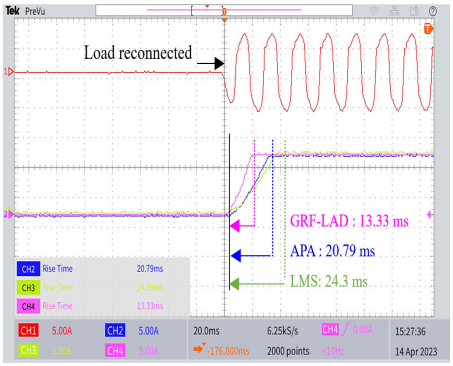

FIGURE 12. Comparison of dynamic response of control algorithms.

when subjected to abrupt load current change. Fig. 12 depicts the control algorithm comparison when the system is subjected sudden reconnection of the load. The APA algorithm and LMS algorithm have a rise time of 20.79 ms and 24.3 ms respectively, while the proposed GRLF-LAD algorithm has considerably less rise time of 13.33ms. So, the GRLF-LAD algorithm is approximately 36.04% faster than APA and about 45.16% faster than LMS in terms of rise time. Thus, it can be seen that the proposed GRLF-LAD algorithm has faster dynamics than the other control algorithms, which results in less latency.

VI. CONCLUSION

The PQ enhancement of an APF that is prepared to function under unstable grid conditions and has resistance to grid-side and load-side disruptions has been shown. The detrimental impacts of harmonically polluted and fluctuating grid voltages from the grid currents have been successfully removed by the QSG-SOGI based grid voltage component extraction. The THD produced by SRF is 12.37%, the THD produced by SOGI is 2.1%, and the THD produced by QSG-SOGI is just 0.08%. In terms of percentage improvement, QSG-SOGI therefore demonstrates a tremendous improvement of about 99.35% over SRF and 96.02% over SOGI. For the purpose of quickly extracting the fundamental weights from the load currents, GRLF-LAD control technique has been used. Under unexpected load disruptions, its response time is fast with good accuracy. The comparison of implemented control algorithm against other controller algorithms provided in the literature has been demonstrated experimentally. The system robustness during load variations, grid voltage sags and swells and grid voltage abnormalities has been ratified experimentally. In terms of dynamic reaction, it is discovered that the GRLF-LAD method is around 36.04% quicker than APA and about 45.16% faster than LMS during load changes and grid voltage irregularities.

VII. FUTURE WORK

With power converters being an indispensable part of the modern power grid, reliable and stable performance of the grid tied system is a crucial area of research. Advanced control strategies are required to ensure stable performance under unbalanced or distorted grid conditions. For future work, APFs employing predictive control and various non-linear control algorithms can be investigated. Furthermore, robust optimization techniques applied to APF control for optimal management of renewable energy sources, gain tuning of controllers can be explored.

APPENDIX A

Simulation Ratings: $C_{DC} = 5000\mu$F, $L_i = 4$ mH, $R_f = 5\Omega$, $C_f = 10\mu$F, $v_G = 220$ V (rms); Sampling time Ts $= 5\mu$s; Experimental Ratings: $V_{DC} = 90$ V; $v_G = 40$ V (rms); $R_f = 15\Omega$, $C_f = 10\mu$F, $L_i = 5$ mH, $k_{pV} = 0.004$ and $k_{iV} = 0.01$; Sampling time Ts $= 60\mu$s;

APPENDIX B

See Table 1.

TABLE 1. Control algorithm parameters.

Algorithm	Parameters
GRF-LAD	$\mu = 0.0175, \tau = 0.94$
APA	μ =0.015
LMS	$\mu = 0.001$
SOGI	k=0.32
QSG-SOGI	$k_{ed} = 100$

REFERENCES

[1] R. Kumar and H. O. Bansal, "Shunt active power filter: Current status of control techniques and its integration to renewable energy sources," *Sustain. Cities Soc.*, vol. 42, pp. 574–592, Oct. 2018.
[2] L. H. Tey, P. L. So, and Y. C. Chu, "Improvement of power quality using adaptive shunt active filter," *IEEE Trans. Power Del.*, vol. 20, no. 2, pp. 1558–1568, Apr. 2005.
[3] G. d. S. Fischer, A. Mengatto, L. G. Kremer, and M. Mezaroba, "A control strategy for a series APF with critical-load-bus voltage feedback that avoids injection transformer saturation," *IEEE Trans. Ind. Appl.*, vol. 55, no. 3, pp. 2290–2299, May 2019.
[4] A. A. Smadi, M. F. Allehyani, B. K. Johnson, and H. Lei, "Power quality improvement utilizing PV-UPQC based on PI-SRF and PAC controllers," in *Proc. IEEE Power Energy Soc. Gen. Meeting (PESGM)*, Denver, CO, USA, Jul. 2022, pp. 1–5.
[5] N. Geddada, M. K. Mishra, and M. V. Manoj Kumar, "SRF based current controller using PI and HC regulators for DSTATCOM with SPWM switching," *Int. J. Electr. Power Energy Syst.*, vol. 67, pp. 87–100, May 2015.

[6] V. Yadav, B. Singh, and A. Verma, "Self-reliant solar PV based microgrid with seamless transition capabilities at weak grid conditions," *Electr. Power Syst. Res.*, vol. 214, Jan. 2023, Art. no. 108825.

[7] B. Singh and S. R. Arya, "Implementation of single-phase enhanced phase-locked loop-based control algorithm for three-phase DSTATCOM," *IEEE Trans. Power Del.*, vol. 28, no. 3, pp. 1516–1524, Jul. 2013.

[8] R. K. Agarwal, I. Hussain, and B. Singh, "Application of LMS-based NN structure for power quality enhancement in a distribution network under abnormal conditions," *IEEE Trans. Neural Netw. Learn. Syst.*, vol. 29, no. 5, pp. 1598–1607, May 2018.

[9] N. Beniwal, I. Hussain, and B. Singh, "Implementation of the DSTATCOM with an i-PNLMS-based control algorithm under abnormal grid conditions," *IEEE Trans. Ind. Appl.*, vol. 54, no. 6, pp. 5640–5648, Nov. 2018.

[10] S. Kumar, B. Singh, and D. Jaraniya, "Multimode features of CIPNLMS-MFX controlled single-phase PV system with finite state machine based islanding/synchronization under grid outage," *IEEE Trans. Ind. Appl.*, vol. 58, no. 2, pp. 1531–1542, Mar. 2022.

[11] M. Bhunia and B. Subudhi, "A self-tuning adaptive control scheme for a grid-connected three-phase PV system," *IEEE J. Emerg. Sel. Topics Power Electron.*, vol. 10, no. 5, pp. 5709–5716, Oct. 2022.

[12] S. R. Arya, K. D. Mistry, and P. Kumar, "Least mean mixed norm square/fourth adaptive algorithm with optimized FOPID gains for voltage power quality mitigation," *IEEE J. Emerg. Sel. Topics Power Electron.*, vol. 11, no. 3, pp. 2632–2640, Jun. 2023.

[13] R. K. Agarwal, I. Hussain, and B. Singh, "LMF-based control algorithm for single stage three-phase grid integrated solar PV system," *IEEE Trans. Sustain. Energy*, vol. 7, no. 4, pp. 1379–1387, Oct. 2016.

[14] M. Srinivas, I. Hussain, and B. Singh, "Combined LMS-LMF-based control algorithm of DSTATCOM for power quality enhancement in distribution system," *IEEE Trans. Ind. Electron.*, vol. 63, no. 7, pp. 4160–4168, Jul. 2016.

[15] A. Bamigbade and V. Khadkikar, "Extended state-based OSG configurations for SOGI PLL with an enhanced disturbance rejection capability," *IEEE Trans. Ind. Appl.*, vol. 58, no. 6, pp. 7792–7804, Nov. 2022.

[16] M. Golla, S. Thangavel, S. P. Simon, and N. P. Padhy, "A novel control scheme using UAPF in an integrated PV grid-tied system," *IEEE Trans. Power Del.*, vol. 38, no. 1, pp. 133–145, Feb. 2023.

[17] V. Saxena, N. Kumar, B. Singh, and B. K. Panigrahi, "An MPC based algorithm for a multipurpose grid integrated solar PV system with enhanced power quality and PCC voltage assist," *IEEE Trans. Energy Convers.*, vol. 36, no. 2, pp. 1469–1478, Jun. 2021.

[18] B. Singh, N. Kumar, and B. K. Panigrahi, "Steepest descent Laplacian regression based neural network approach for optimal operation of grid supportive solar PV generation," *IEEE Trans. Circuits Syst. II, Exp. Briefs*, vol. 68, no. 6, pp. 1947–1951, Jun. 2021.

[19] A. Sharma, B. S. Rajpurohit, and S. Agnihotri, "Affine projection sign algorithm based control for mitigation of distribution side power quality problems," *Energy Convers. Econ.*, vol. 2, no. 2, pp. 79–90, Jun. 2021.

[20] A. H. Sayed, *Fundamentals of Adaptive Filtering*. Hoboken, NJ, USA: Wiley, 2003.

[21] W. Liu, P. P. Pokharel, and J. C. Principe, "Correntropy: Properties and applications in non-Gaussian signal processing," *IEEE Trans. Signal Process.*, vol. 55, no. 11, pp. 5286–5298, Nov. 2007.

[22] B. Chen, L. Xing, H. Zhao, N. Zheng, and J. C. Príncipe, "Generalized correntropy for robust adaptive filtering," *IEEE Trans. Signal Process.*, vol. 64, no. 13, pp. 3376–3387, Jul. 2016.

[23] F. Huang, J. Zhang, and S. Zhang, "Maximum versoria criterion-based robust adaptive filtering algorithm," *IEEE Trans. Circuits Syst. II, Exp. Briefs*, vol. 64, no. 10, pp. 1252–1256, Oct. 2017.

[24] X. Yu, J. Liu, and H. Li, "An adaptive inertia weight particle swarm optimization algorithm for IIR digital filter," in *Proc. Int. Conf. Artif. Intell. Comput. Intell.*, Shanghai, China, Nov. 2009, pp. 114–118.

[25] M. O. Sayin, N. D. Vanli, and S. S. Kozat, "A novel family of adaptive filtering algorithms based on the logarithmic cost," *IEEE Trans. Signal Process.*, vol. 62, no. 17, pp. 4411–4424, Sep. 2014.

[26] K. Xiong and S. Wang, "Robust least mean logarithmic square adaptive filtering algorithms," *J. Franklin Inst.*, vol. 356, no. 1, pp. 654–674, Jan. 2019.

[27] O. M. Abdelrhman, Y. Dou, and S. Li, "A generalized robust logarithmic family-based adaptive filtering algorithms," *IEEE Trans. Circuits Syst. II, Exp. Briefs*, vol. 70, no. 8, pp. 3199–3203, Aug. 2023.

[28] J. K. Singh, K. A. Jaafari, R. K. Behera, K. A. Hosani, and U. R. Muduli, "Faster convergence controller with distorted grid conditions for photovoltaic grid following inverter system," *IEEE Access*, vol. 10, pp. 29834–29845, 2022.

[29] A. A. Smadi, H. Lei, and B. K. Johnson, "Distribution system harmonic mitigation using a PV system with hybrid active filter features," in *Proc. North Amer. Power Symp. (NAPS)*, Wichita, KS, USA, Oct. 2019, pp. 1–6.

[30] M. K. Mishra and V. N. Lal, "A multiobjective control strategy for harmonic current mitigation with enhanced LVRT operation of a grid-tied PV system without PLL under abnormal grid conditions," *IEEE J. Emerg. Sel. Topics Power Electron.*, vol. 11, no. 2, pp. 2164–2177, Apr. 2023.

[31] S. Tyagi, B. Singh, and S. Das, "ELD-OSG control of a battery-based electronic load controller for a small hydro energy conversion system," *IEEE Trans. Ind. Appl.*, vol. 58, no. 3, pp. 3142–3152, May 2022.

[32] S. Das and B. Singh, "Flexible ripple minimization technique for wind-solar renewable energy system under unbalanced and distorted grid conditions," *IEEE Trans. Ind. Appl.*, vol. 58, no. 5, pp. 6739–6751, Sep. 2022.

[33] Y. Singh, B. Singh, and S. Mishra, "An uninterruptable PV array-battery based system operating in different power modes with enhanced power quality," *IEEE Trans. Ind. Electron.*, vol. 69, no. 4, pp. 3631–3642, Apr. 2022.

[34] R. K. Lenka, A. K. Panda, R. Patel, and J. M. Guerrero, "PV integrated multifunctional off-board EV charger with improved grid power quality," *IEEE Trans. Ind. Appl.*, vol. 58, no. 5, pp. 5520–5532, Sep. 2022.

[35] M. Badoni, A. Singh, S. Pandey, and B. Singh, "Fractional-order notch filter for grid-connected solar PV system with power quality improvement," *IEEE Trans. Ind. Electron.*, vol. 69, no. 1, pp. 429–439, Jan. 2022.

[36] S. Mohamadian, H. Pairo, and A. Ghasemian, "A straightforward quadrature signal generator for single-phase SOGI-PLL with low susceptibility to grid harmonics," *IEEE Trans. Ind. Electron.*, vol. 69, no. 7, pp. 6997–7007, Jul. 2022.

MASIHA AIJAZ received the M.Tech. degree in electrical power system management from Jamia Millia Islamia, New Delhi, India, in 2018. She is currently pursuing the Ph.D. degree in electrical engineering with the Department of Electrical Engineering, National Institute of Technology Srinagar, India. Her research interests include power electronics, power quality, custom power devices, renewable energy systems, power quality improvement in distribution networks, renewable energy based electric vehicle charging, and adoption of optimisation algorithms in electric vehicle charging applications.

IKHLAQ HUSSAIN (Senior Member, IEEE) received the B.E. degree in electrical from the University of Jammu, Jammu, India, in 2009, the M.Tech. degree (Hons.) in electrical power system management from Jamia Millia Islamia (A Central University), New Delhi, India, in 2012, and the Ph.D. degree from the Department of Electrical Engineering, Indian Institute of Technology Delhi, New Delhi, in 2018. From 2018 to 2022, he was an Assistant Professor with the Department of Electrical Engineering, University of Kashmir, Jammu and Kashmir, India. From July 2022 to September 2022, he was a Research Fellow with the National University of Singapore. Since November 2022, he has been an Assistant Professor with the Department of Electrical Engineering, National Institute of Technology Srinagar, Jammu and Kashmir. He has coauthored more than 180 journals and conference papers. His research interests include power electronics, power quality, custom power devices, renewable energy systems, optimisation algorithms, electric vehicle charging, and microgrids. He is a fellow of the Institution of Electronics and Telecommunication Engineers (IETE). He was a recipient of the POSOCO Power System Award (PPSA), the Gandhian Young Innovations Award in 2018, and the Outstanding Faculty Researcher in the field of energy for 2017 and 2018. He has participated as a Young Scientist in third BRICS Young Scientist Conclave by the Department of Science and Technology, Government of India, Durban, South Africa, from 25th to 29th June 2018. He has filed three patents and awarded two national patents. He has been featured thrice in the Stanford list of world's top 2% researchers in the field of energy. He is serving as an Associate Editor for *The International Journal of Power and Energy Systems* (ACTA Press) and *International Journal of Circuit Theory and Applications* (Wiley Publishers).

SHAMEEM AHMAD LONE (Member, IEEE) received the M.E. degree (Hons.) from the Indian Institute of Technology Roorkee, Roorkee, India, in 1998, and the Ph.D. degree in electrical engineering from the National Institute of Technology Srinagar, Srinagar, India, in 2007. Since 1994, he has been with the Department of Electrical Engineering, National Institute of Technology Srinagar, where he is currently a Senior Professor. He has published more than 50 research papers in reputed national and international journals and conference proceedings. His research interests include stand-alone power systems, hybrid and weak power systems, role of energy storage in improving the power quality, and intelligent control techniques. He is a fellow of The Institution of Engineers, India.

MUKUL CHANKAYA received the B.Tech. degree in electrical engineering from Kurukshetra University, Kurukshetra, Haryana, India, in 2008, the M.Tech. degree in power system and design from the YMCA University of Science and Technology, Faridabad, Haryana, in 2012, and the Ph.D. degree from the National Institute of Technology Srinagar, India, in 2022. He was an Assistant Professor with Lovely Professional University, Punjab, India, from 2012 to 2017. Since 2022, he has been an Assistant Professor with the School of Electrical Engineering, Vellore Institute of Technology, Vellore, India. His research interests include renewable energy systems, power electronics, power quality, and optimization. He was a recipient of the IEEE SCES 2020 Best Paper Award in 2020.